P1.5 NUMERICAL STUDY OF URBAN GROWTH EFFECTS ON SURFACE ATMOSPHERIC FIELDS OVER A COASTAL TROPICAL CITY

Pedro J. Mulero*, Alexander Velázquez, Jorge E. González, and Amos Winter

University of Puerto Rico, Mayagüez, Puerto Rico

1. INTRODUCTION

1.1 *Overview of the San Juan UHI*

Puerto Rico is the easternmost of the Greater Antilles. Its center is roughly located at 18.20° north-latitude and 66° west-longitude. The island has almost a rectangle-like shape with a length of 180 km and 56 km width for a total area of 10,080 km^2. San Juan, its capital, has a metropolitan area of ~3,000 km^2 with over 2 million people within its boundaries. The city is located at the northeastern coast of the island and is under the quasi-perennial influence of the synoptic scale trade winds, which blow mainly from the east to the east-northeast. The mesoscale sea-breeze circulation also modulates temperatures and flow over the city, particularly during the summer, when trade winds are lighter and surface heating is greater.

At smaller scales, however, observations indicate that the large urban landscape and continued expansion might influence to some extent local weather across the area. Figure 1 shows how surface temperatures for the month of January (one of the driest climatologically) have been increasing, albeit slightly (~0.035°C year^{-1}), for the past several decades over the downtown section of the city. Whether this is an island-wide related trend caused by long time-scale climatological patterns or an urban-associated increase remains to be studied further.

Data from the Advanced Very High Resolution Radiometer (AVHRR), onboard a NOAA-Satellite, was retrieved to calculate the Normalized Difference Vegetation Index (NDVI) and the Apparent Surface Temperature (APST). The AVHRR sensor is a broadband five-channel scanner, which senses in the visible, near infrared,

*Corresponding author address:
Pedro J. Mulero, UPRM, Dept. of Mechanical Enginnering, Puerto Rico, 00680; e-mail: pmulero@me.uprm.edu.

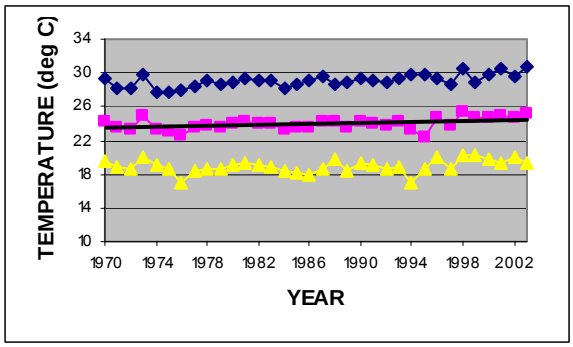

Figure 1: Time-series analysis for downtown San Juan temperatures on January (in °C). Blue, pink, and yellow lines depict maximum, average and minimum temperatures, respectively. The solid black line represents a linear regression on the average temperatures.

and thermal infrared portions of the electromagnetic spectrum, the radiative emission off the surface. The variables NDVI and AST are calculated combining the data collected from the different channels of the sensor using a set of simple equations (not shown here). Results from the calculation of the NDVI can be seen in Figure 2. Values range from 0.0 to 0.5, which represent non-vegetated to well-vegetated areas, respectively. An area corresponding to the urbanized area of San Juan can be identified as one of the non-vegetated areas in the image.

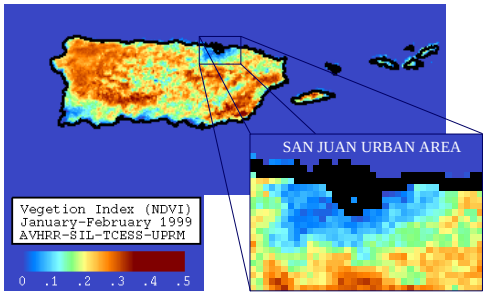

Figure 2: Negative difference vegetation index (NDVI); from data of NOAA satellite using the AVHRR sensor on January-February, 1999.

Figure 3 shows the APST for 0400AST 7 April 1998. The scale observed in the legend goes from 40°C to –40°C. The darker areas represent the higher temperatures whereas the whiter areas represent the presence of clouds in the image. The calculated APST reveals a hot spot over the urbanized area of San Juan, which contrasts with the lower temperatures detected immediately away from the city. All these observations suggest the urban growth over the city is directly influencing surface temperatures, and more than likely, many other atmospheric variables such as wind flow and precipitation. Observational and modeling studies of urban-induced convective activity are documented in Bornstein and Lin (2000), Rozzoff (2002), Shepherd and Burian (2003), to name only a few.

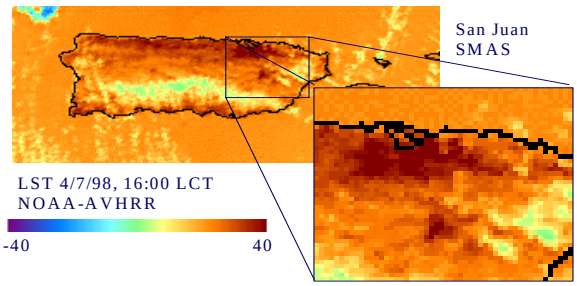

Figure 3: Apparent surface temperature (APST), from NOAA satellite data using the AVHRR sensor on April 7, 1998 at 4:00 pm AST.

1.2 *Previous Work*

Velazquez et al. (2002) demonstrated the existence of the Urban Heat Island (UHI) effect over San Juan by performing a series of fake-dry numerical experiments in which the thermal and mechanical characteristics of soil were configured differently for each one. In his experiment, he constructs three scenarios: 'primitive', current, and future, each one with varying degrees of soil and land use characteristics. He concluded that the intensity of the San Juan UHI -measured by the temperature difference between the urban and rural areas- is bound to increase at a rate of 0.06° $year^{-1}$ if we expand the urban landscape of San Juan at a linear rate in relation to the population growth expected for 2050 (i.e. the future case).

Hafner and Kidder (1998) employed a three-dimensional model to simulate the UHI effect. They retrieved surface parameters from AVHRR satellite data, such as albedo and soil thermal and moisture properties, to incorporate these into their modeling tasks. Martilli (2002) used a 2-D mesoscale model to study the effects of urban morphology (using different urban configurations with varying building heights), wind speed, and rural soil moisture, on the boundary layer structure.

In this work, a primitive equation, non-hydrostatic mesoscale model is used to study the effects of change land surface characteristics on surface atmospheric conditions over the city of San Juan, Puerto Rico, and its nearby rural surroundings. To accomplish our goals, two different land cover-land use (LCLU) scenarios are tested, each with a different amount of horizontal urban mass. A control simulation (CTL) uses the standard vegetation data files already provided by the mesoscale model, which depict an urban mass of about 110km^2. The second experiment, which actually resembles the current urban mass of the city (based on recent airborne satellite data), triples the urban landscape to around 330km^2. We will refer to the latter scenario as the Extended-Urban case (EU). The output from these experiments will be used to analyze the effects of each LCLU configuration on several surface momentum and thermodynamic fields.

A second part of this project, still underway, focuses on conducting experiments in which a moisture perturbation is added to the eastern half of Puerto Rico at initialization, using the same two LCLU scenarios. These experiments will study the triggering of the onset of convection across the area with particular emphasis on the location, intensity, and structure of the convective activity.

2. NUMERICAL EXPERIMENTS

2.1 *Model configuration*

Numerical experiments in this study are conducted using the CSU/MRC-ASTeR Regional Atmospheric Modeling System (RAMS), version 4.3 (Cotton et al. 2003). A two-way interactive doubly nested-grid technique is employed to achieve the multiscale simulations. The outer mesh has (x,y) dimensions of 64 x 34 grid points with a horizontal grid spacing of 64km. The middle and innermost meshes have dimensions of 86 x 58 and 78 x 34 points, respectively. All grids contain 54 vertical levels (non-dimensional sigma levels). The finest mesh focuses on the island of Puerto Rico (refer to Fig. 4 for the grid configuration). The 54 vertical levels are spaced so that higher resolution is provided in the planetary boundary layer (PBL) than at the upper

levels with the model top at ~24km. Bottom boundary conditions are provided by standard sea surface temperature (SST) and vegetation/land cover datasets already prepared and integrated to the model. Data from the United States Department of Agriculture (USDA) was used to provide detailed soil type data for Puerto Rico at the 4km grid spacing domain. The same soil type was assigned homogenously to the entire soil column, which has a 50cm depth with 11 layers.

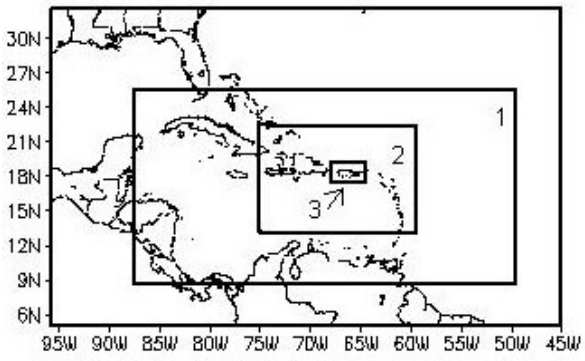

Figure 4: RAMS grid configuration.

A land surface model, LEAF-2 (Land Ecosystem-Atmosphere Feedback) (Walko et al. 2000), is coupled to the atmospheric model. Soil moisture is initialized at 15% in all our experiments. The radiation scheme of Mahrer and Pielke (1977) and the convective parameterization of Kuo (1974) are used in all three simulations. The Mellor and Yamada scheme takes care of the parameterization of vertical diffusion (Mellor and Yamada, 1982).

2.2 *Modeling exercises*

Velazquez et al. (2002) showed that 2-m height temperature differences between the urban areas and its rural surroundings (i.e. intensity of the urban heat island) increase progressively from the 'primitive' state to the 'current' and then a 'future' case scenario. His 'future' scenario, as he calls it, employs a much larger urban landscape than the one used in this study. A broader treatment of surface atmospheric fields, both dynamic and thermodynamic, as related to the urban growth of a large coastal city located on a tropical setting, is the main driver of this work. A control (CTL) simulation is developed in which the standard vegetation files provided by RAMS are left unchanged for the entire island. A ~110km^2 urban area is calculated based on the model's interpolation of vegetation files into the 4km grid spacing domain. An extended-urbanized (EU) area simulation is done by increasing the horizontal growth of urban material to ~330km^2, tripling the amount from the control run. Experiments are initialized on 0000UTC 23 January 1998 and integrated over 48h. Analysis is primarily done during the peak surface heating hours. NCEP Reanalysis data (Kalnay et al., 1996) provides the lateral boundary conditions at every 6h. These 48h time period was chosen to be a dry, synoptically unperturbed period.

3. RESULTS

Figure 5 shows a very similar structure of maximum and minimum temperature values between the CTL and EU simulations. However, a direct cell-by-cell comparison indicates a tendency for cooler temperatures in the coastal and near-coastal sections of San Juan is seen when the urban area is expanded (Fig. 5e). However, maximum temperatures tend to increase in the south-central region of the city. This means there is an increase in the north-south temperature gradient over the city when the urban landscape is expanded. An enhanced oceanic influence might act to slightly cool temperatures in the immediate

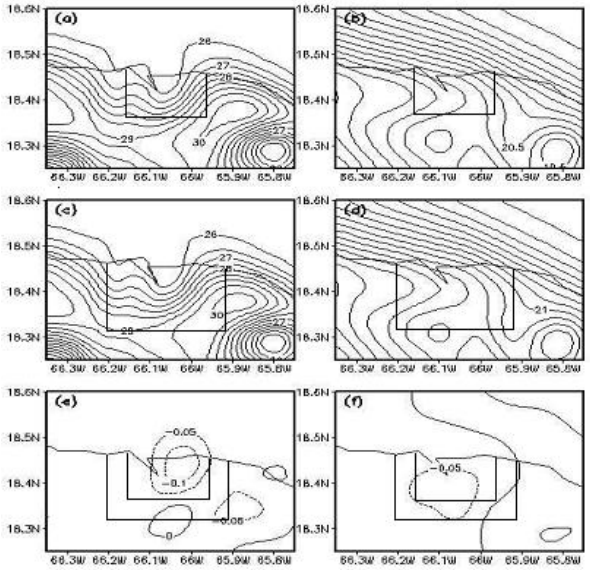

Figure 5: CTL simulation 2-m height (a) maximum and (b) minimum temperatures (at every 0.5 deg C) for 25 January 1998 over the San Juan area; EU (c) maximum and (d) minimum temperatures; (e) maximum and (f) minimum temperature differences (EU – CTL) at 0.05 deg C intervals. The 1500-1900UTC (1100-1500AST) and 0600-1000UTC (0200-0600AST) periods were chosen to determine the maximum and minimum

temperatures. Boxes depict urban areas for both runs.

coastal areas. Wind flow (i.e. meridional or onshore component of the wind), however, decreases (not shown). The equivalent potential temperature field (θ_e) does not support this hypothesis as it shows lower θ_e values in the coastal areas for the EU scenario (not shown), in contrast to what would be expected under warm, moist, enhanced on-shore flow.

The minimum temperature field shows less variability from one run into the other (Fig. 5f). Still, a pocket of cooler temperatures is seen in the central parts of the city when examining the EU – CTL run field. This is likely due to the drier (i.e. less amounts of water vapor) conditions over the city at this early morning period as seen in Figure 6 showing the difference EU – CTL equivalent potential temperature (θ_e). The θ_e field has slightly decreased right over most of the area of interest during the early morning hours. EU – CTL θ_e values turn smaller as they get closer to the coast and into the open ocean, as we would expect. Figure 7 also shows a decreased wind speed field when expanding the urban zone, allowing for radiational cooling to take place more effectively.

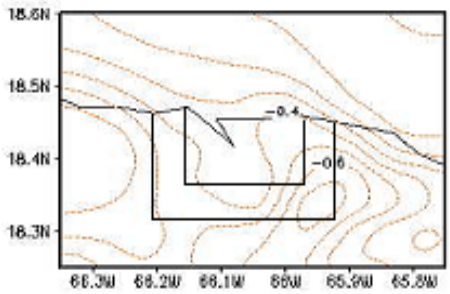

Figure 6: EU – CTL average surface theta-e field for the 0600-1000UTC (0200-0600AST) 25 January 1998 period at 0.1K intervals. Solid (dashed) contours show positive (negative) values.

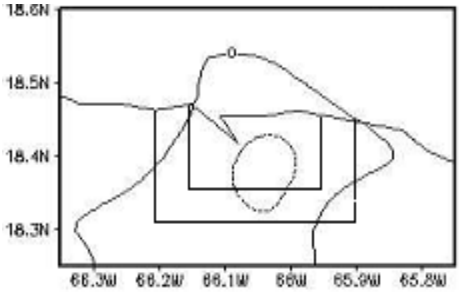

Figure 7: Same as Fig. 7 but for the EU – CTL average wind speed difference at 0.1 m s-1 intervals.

An inspection of surface wind vectors, an easterly trade flow prevails over the open ocean and just offshore of the city for both simulations (Fig. 8a-b). Both sea breeze and land frictional effects account for the backing of the wind direction. Wind, however, loses its onshore component as it encounters topographically driven airflow (one of the island's highest peaks is at the southeast corner of the figure domain). A more detailed flow discussion is beyond the scope of this work.

Wind speed analysis shows a decrease in wind speed in the EU simulation, as compared to the CTL run during the 1100-1500AST period. A sink in the momentum field is mainly present across the entire enhanced urbanized area, mainly in the central sectors. Coastal areas show a decrease in wind speed in the –0.1 to –0.2 m s-1 range whereas interior parts of the city depict values reaching –0.6 m s-1. This general pattern of flow decrease can be due, as suggested earlier, to the increased drag imposed by the enhanced urban roughness across the area. Land surface frictional effects, as well as the afternoon onset of the sea breeze circulation, deflect the easterly flow over the ocean into a more northeasterly fashion. See breeze appears to be weak, but can be easily depicted on an island-wide streamline analysis (not shown).

A look at the surface divergence pattern shows a general area of negative surface divergence (i.e. convergence) across the entire urbanized area, as
would normally be expected during the peak hours of solar insolation (Fig. 9). The central part of the urban area and a rural zone downwind of the city are where localized maxima of stronger convergence occur. Divergence is more common close to the coastal areas where airflow is still being unaffected by the increased surface roughness of the urban territory. This convergence pattern in the inner San Juan area does not seem to be thermally driven (i.e. due to thermal contrasts between the urban and rural areas), but the consequence of easterly flow deceleration as air transfers its path from an oceanic surface, with relatively low friction, to a much more frictional urban landscape. Weaker convergence is evident over the heart of the city as we expand the urbanized San Juan area. This

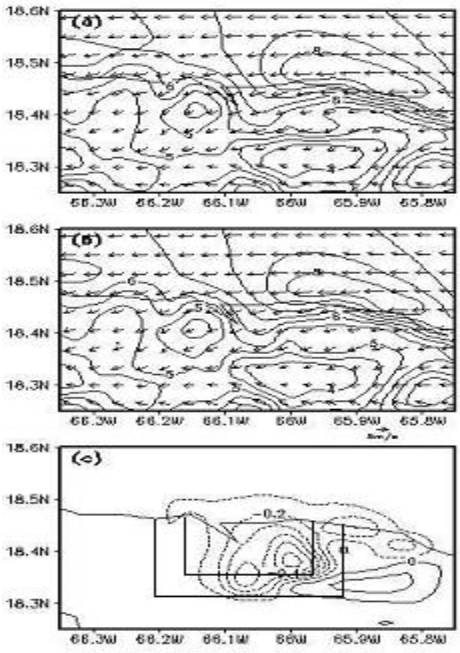

Figure 8: 1500-1900UTC (1100-1500AST) 25 January 1998: Average wind speed in m s-1 (at every 0.5 m s-1) and vectors for (a) CTL and (b) EU simulations; (c) shows differences in wind speed (EU – CTL) at 0.1 m s-1 intervals.

is likely due to the weaker interaction of the northeasterly flow over the city with the topographically induced flow to the south of the area, which has a slight northward component. The tendency is reversed upstream of the city, where convergence is enhanced from the CTL to

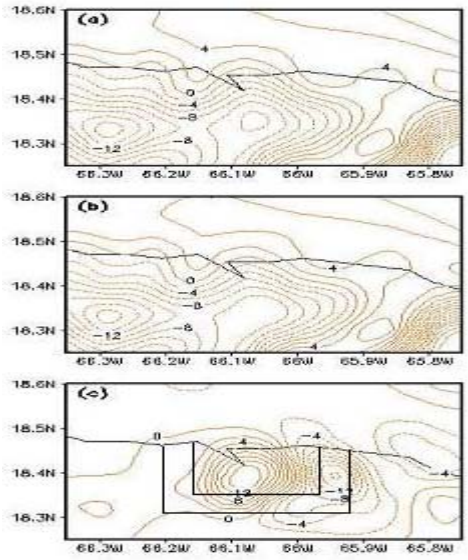

Figure 9: Contours represent surface divergence in 10^{-4} s^{-1} units on 1800UTC (1400AST) 25 January 1998 for (a) CTL and (b) EU simulations; (c) shows the divergence difference (EU – CTL). Contours for (a) and (b) are drawn at $2x10^{-4}$ s^{-1} intervals and at every $2x10^{-5}$ s^{-1} for (c).

the EU simulation. This is likely due to the addition of urban land use to the east of the original CTL run, causing the damping effects on the dynamic field explained above.

4. SUMMARY AND CONCLUSIONS

A simple analysis on the behavior of several surface dynamical and thermodynamical atmospheric fields as a function of increased urbanized area have been addressed on this study for San Juan, Puerto Rico. Mechanical factors, such as the walls and heights of the buildings, as well as human-induced thermal factors, have been ignored. A conventional approach of parameterizing the thermo-mechanical properties of urban land use has been used.

Two simulations were conducted to achieve our results. A control (CTL) run and an extended-urbanized (EU) simulation, the latter having a significant increase in urban mass in compared to the former, were performed. Daylight maximum temperatures were higher in the EU run over the inner-most parts of the city, but cooler in the coastal sections. The cause for this disparity is still unknown, which poses a question for further work. Minimum temperatures are cooler in the center of the urban area for the EU run as lighter winds and drier conditions prevail away from the coast. Wind flow is generally slower over the entire domain when urban land replaces a significant portion of vegetated area present in the CTL experiment. A decrease in surface convergence occurs in the core of the urban area when looking at the EU run, as compared with the CTL case, probably because flow over the central San Juan area does not decelerate as much in the EU simulation as it finds less resistance from topographically driven flow with a slight northward component which has itself decelerated once it encounters a higher surface roughness to the south of where it was originally placed in the CTL run. Convergence is enhanced, however, in the eastern quarter of the expanded urban zone as flow is suddenly forced to decelerate also due to increased surface roughness, this time to the east of the original case.

These results certainly challenge the hypothesis of an increasing intensity of the UHI over San Juan induced by strict urban landscape

increase without including the anthropogenic factor. Both synoptic and mesoscale dynamics seem to control surface atmospheric conditions over the city of San Juan and offset any urban-induced increase in temperatures. More intense modeling efforts are needed to prove these conclusions.

Further work will include a more in-depth analysis of several other surface atmospheric fields for these two cases that can explain how the momentum and thermodynamic fields are altered when a piece of urban mass is added to a large city located on a tropical setting. A look at more different scenarios on land use over this same area (e.g. removing all urban land use) will be examined in future modeling studies. A study on how convective activity is enhanced or halted by increasing the urban landscape, by adding a θ_e perturbation at initialization on a specified domain (including both the city and a large area of the surrounding rural areas), is also underway.

5. REFERENCES

Bornstein, R., and Q. Lin, 2000: Urban heat islands and summertime convective thunderstorms in Atlanta: Three case studies. *Atmos. Environ.*, **34**, 507-516.

Cotton, W.R., and Coauthors, 2003: RAMS 2001: Current status and future directions. *Meteor. Atmos. Phys.*, **82**, 5-29.

Hafner J., and S. Q. Kidder, 1998: Urban heat island modeling in conjunction with satellite-derived surface/soil parameters. *J. Appl. Meteor*., **38**, 448-465.

Kalnay E., M. Kanamitsu, R. Kistler, W. Collins, D. Deaven, J. Derber, L. Gandin, S. Sara, G. White, J. Woollen, Y. Zhu, M. Chelliah, W. Ebisuzaki, W. Higgins, J. Janowiak, K.C. Mo, C. Ropelewski, J. Wang, M.A. Leetman, R. Reynolds, and R. Jenne, 1995: The NMC/NCAR reanalysis project. *Bull. Amer. Meteor. Soc.,* **77,** 437-471.

Kuo, H.L., 1974: Further studies of parameterization of the influence of cumulus convection on large scale flow. *J. Atmos. Sci*., **31**, 1232- 1240.

Mahrer, Y. A., and R.A. Pielke, 1977: A numerical study of the airflow over irregular terrain. *Beitrage Physik der Atmosphare.***, 50,** 98-113.

Shepherd, J.M., and S.J. Burian, 2003: Detection of urban-induced rainfall anomalies in a major coastal city*. Earth Interactions,* **7,** 1-15.

Martilli, A., 2002: Numerical study of urban impact on boundary layer structure: Sensitivity to wind speed, urban morphology, and rural soil moisture. *J. Appl. Meteor*., **41**, 1247-1266.

Mellor, G.L., and T. Yamada, 1982: Development of a turbulence closure model for geophysical fluid problems. *Rev. Geophys. Space Phys.*, **20**, 851-875.

Rozoff, C.M., W.R. Cotton, and J.O. Adegoke, 2002: Simulation of St. Louis, Missouri, land use impacts on thunderstorms. *J. Appl. Meteor*., **42**, 716-738.

Tripoli, G. J., and W. R. Cotton, 1982: The Colorado State University three-dimensional cloud/mesoscale model – 1982. Part I: General theoretical framework and sensitivity experiments. *J. de Rech. Atmos.*, **16**, 185-220.

Velazquez, A., A. Winter, and J.E. Gonzalez, 2002: Urban heat island analysis over San Juan, Puerto Rico. *Submitted for publication to the J. Appl. Meteor.*

Walko R.L., L.E. Band, J. Baron, T. G. F. Kittel, R. Lammers, T.J. Lee, D. Ojima, R.A. Pielke, C. Taylor, C. Tague, C.J. Tremback, and P.J. Vidale, 2000: Coupled atmosphere-biophysics-hidrology models for environmental modeling*. J. Appl. Meteor.,* **39**, 931-944.